Journal of Membrane Science 520 (2016) 657–670

Contents lists available at ScienceDirect

Journal of Membrane Science

journal homepage: www.elsevier.com/locate/memsci

Simultaneous unzipping and sulfonation of multi-walled carbon nanotubes to sulfonated graphene nanoribbons for nanocomposite membranes in polymer electrolyte fuel cells

Avanish Shukla [a,b], Santoshkumar D. Bhat [a,b,*], Vijayamohanan K. Pillai [a,b]

[a] Academy of Scientific and Innovative Research (AcSIR), CSIR - Central Electrochemical Research Institute (CSIR-CECRI) Campus, Karaikudi, India
[b] CSIR - Central Electrochemical Research Institute - Madras Unit, CSIR Madras Complex, Chennai, India

ARTICLE INFO

Article history:
Received 21 February 2016
Received in revised form
23 July 2016
Accepted 14 August 2016
Available online 15 August 2016

Keywords:
Multi-walled carbon nanotubes
Sulfonated graphene nanoribbons
Nanocomposite membrane
Proton exchange membrane fuel cells

ABSTRACT

Simultaneous in situ unzipping and sulfonation of multi-walled carbon nanotubes (MWCNTs) using potassium sulfate (K_2SO_4) and sodium dodecyl benzene sulfonate (SDBS) by a hydrothermal synthetic route is carried out to prepare sulfonated graphene nanoribbons (sGNR) as confirmed by various characterization techniques. Further, nanocomposite polymer electrolyte membranes of this with sulfonated polyether ether ketone (SPEEK) show enhanced ion exchange capacity (IEC), proton conductivity and water uptake compared to that of pristine SPEEK membrane. Higher mechanical stability for these composite membranes is observed in comparison with pristine SPEEK membrane. Interestingly, these SPEEK/sGNR composite electrolyte membranes (0.1 wt% sGNR) while testing in a proton exchange membrane fuel cell (PEMFCs) test-bed, shows a current density of 840 mA cm^{-2} at 0.6 V (peak power density of 660 mW cm^{-2}) compared to the current density of 480 mA cm^{-2} at 0.6 V (peak power density of 331 mW cm^{-2}) for pristine SPEEK. The accelerated durability test for the membranes confirms that composite membranes of SPEEK/sGNR are highly durable even after 200 h with marginal drop in OCV with negligible fuel cross-over up to 175 h to suggest its potential applications in slew of future technologies including polymer electrolyte fuel cells, water electrolyzers and electrochemical sensors.

1. Introduction

Generation, storage and convenient retrieval of clean energy is a primary concern of almost all countries and fuel cells are widely known to tackle most of the issues associated with it, being an intrinsically efficient and clean energy conversion device [1,2]. Among several types of fuel cells, polymer electrolyte membrane fuel cells (PEMFCs) with its zero emission characteristics and modularity are especially suitable for both transport as well as stationary applications [3,4] despite many serious issues associated with affordability. Membrane electrode assembly (MEA) in PEMFCs plays an important role in determining the cell performance and most of the research is focused on developing new membrane electrolytes and electrocatalysts [5,6] using both inexpensive materials and cheaper manufacturing practices compatible for scale-up and production.

At present, perfluorosulfonic acid polyelectrolyte, Nafion, is widely used as a membrane electrolyte for PEMFCs due to its high ionic conductivity and long term stability [1,7]. However, since cost being a major concern of Nafion, research efforts are directed towards exploring alternative polymers to be used as electrolyte for PEMFCs [1,7]. Poly(ether ether ketone) (PEEK) polymer is a semi-crystalline polymer [8] and being cost effective is considered to be a best available alternative option to match the characteristics of Nafion in terms of chemical, mechanical and thermal stability and can be sulfonated using lesser carcinogenic reagents [3,9]. Other advantages in terms of low fuel permeability are also associated with sulfonated Poly (ether ether ketone) (SPEEK) [10]. However, a higher degree of swelling in SPEEK with increased degree of sulfonation and ionic conductivity are some of the important challenges that needs to be addressed when used as electrolyte in PEMFCs [9]. The thermal stability of SPEEK also depends on the degree of sulfonation (DS) as it increases the proton conductivity but at very high DS, thermal and mechanical stability get affected significantly [10]. The proton conductivity of SPEEK in turn depends on relative humidity and at high relative humidity and temperature, the degree of membrane swelling increases due to the excess water absorption as the DS increases in SPEEK [10].

* Corresponding author at: CSIR-Central Electrochemical Research Institute-Madras Unit, CSIR Madras Complex, Chennai, India
E-mail address: sdbhat@cecri.res.in (S.D. Bhat).

http://dx.doi.org/10.1016/j.memsci.2016.08.019
0376-7388/

To address above issues, introduction of stable secondary phase is important to form its composites. In this concern, SPEEK and its composites by dispersing different additives are recently explored as electrolytes to enhance the polymer electrolyte fuel cell (PEFC) performance [9]. Some of the important additives like zeolites, functionalized silicates, metal oxides, sulfated zirconia, heteropolyacids and layered silicates to form SPEEK composites are explored in PEFCs [9]. In recent years, carbon nanostructures have been the topic of interest to be used as additive to the polymer matrix for membrane electrolyte in PEFCs because of its remarkable mechanical and thermal properties, low density and high aspect ratio [9,11]. However, structural modification and sulfonation of these materials are important for its better activity and dispersion in the polymer matrix [9,11]. Different types of modified/sulfonated carbon nanostructures like single walled carbon nano-tubes (SWCNTs), MWCNTs, carbon nanospheres, graphene oxide and fullerene have been incorporated as additives to form polymer composite membranes with Nafion and SPEEK as a base polymer to enhance the physico-chemical properties required for a polymer electrolyte membrane (PEM) [12–17]. For instance, Nafion/functionalized CNTs composite membranes with enhanced thermal properties along with increased proton conductivity were reported [13,14]. Similarly, Kannan et al. reported sulfonic acid functionalized single walled-carbon nanotubes (S-SWCNTs) incorporated in Nafion with improved proton conductivity and mechanical stability to form a composite membrane for PEMFCs [12]. Also, functionalized sulfonated MWCNTs/Nafion composite membrane was investigated for the application in PEMFCs with the increased proton conductivity, mechanical characteristics and enhanced fuel cell performance [15]. The composite membranes of sulfonated porous carbon nanospheres with Nafion (Nafion/sPCN) were also explored to increase the ionic conductivity for its use as electrolyte in PEMFCs [16]. Recently, graphene and fullerene based structures are also studied as additives in Nafion and SPEEK. For instance, the composite membranes of sulfonated graphene oxide and Nafion (Nafion/SGO) [17] and sodium dodecyl benzene sulfonate (SDBS)-adsorbed graphene oxide with SPEEK (SPEEK/SDBS-GO) [18] was also investigated for its application in fuel cells. Similarly composite membranes of sulfonated fullerene with SPEEK (SPEEK/Sfu) were also used for better fuel cell performance [19]. However, there are certain limitations in the above approaches in terms of finding more sulfonation sites and structural compatibility for different carbon nanostructures within the polymeric matrix.

In the present study, MWCNTs are in situ unzipped to increase more number of available sulfonation sites and sulfonated simultaneously by adsorbing sulfonic acid (SDBS) groups to form sulfonated graphene nanoribbons (sGNR). This is also essential for proper structural compatibility of sGNR to be incorporated in the SPEEK matrix for composite membrane electrolyte in PEFCs. GNR have more available surface area for sulfonation than MWCNTs which in turn helps in forming more ionic sites during sulfonation for increasing ionic conductivity. Sodium dodecyl benzene sulfonate (SDBS) is used as a sulfonating precursor during unzipping of MWCNTs since it provides the π-π interaction without any structural deformation. Finally, sGNR is dispersed in SPEEK in different wt% ratio (0.05, 0.1 and 0.15) to form composite membrane electrolytes. These are characterized for their physicochemical properties and formed MEAs were subjected to cell polarization. Among these composites, 0.1 wt% of sGNR has shown better dispersion in the polymer matrix. Higher IEC, water uptake, conductivity, mechanical stability and fuel cell performance is observed for SPEEK/sGNR (0.1 wt%).

2. Experimental

2.1. Materials

Multi-walled carbon nanotubes (MWCNTs, ≥98% carbon basis, O.D. × I.D. × L. 10 nm ± 1 nm × 4.5 nm ± 0.5 nm × 3- ~6 μm, 773840-25G) and sodium dodecyl benzene sulfonate (SDBS, 289957-500G) were purchased from Sigma Aldrich. Potassium sulfate (K_2SO_4) was purchased from Sisco research laboratories (SRL) Pvt. Ltd. Sulfonated poly(ether ether ketone) (SPEEK, M_w=50,000 g mol^{-1}, M_n=14,000) was purchased from FuMA-Tech GmbH, Germany. Dimethyl acetamide (DMAc) was procured from Acros organics India. Commercial gas diffusion layer i.e. GDL (SGL-DC-35) was supplied by SIGRACET®, GmbH, Germany. Platinum supported on carbon i.e. Pt/C (40 wt% Pt on Vulcan XC-72R carbon) was purchased from Alfa Aesar (Johnson Matthey, USA) chemicals. All the above mentioned chemicals were used as received without any modification. Nafion 212 membrane was obtained from Dupont and pretreated before PEFC test. Deionized water (DI) (Elix® 10, MERCK MILLIPORE) was used for all the experiments.

2.2. Preparation of SDBS adsorbed graphene nanoribbons (sGNR)

MWCNTs (150 g) were properly mixed in 150 ml DI water under stirring for 1 h. 0.5 M K_2SO_4 was added to the above solution and was further sonicated for 1 h [20]. 0.016 M SDBS (0.873 g) with pH=1.77 was added to the above dispersion and again sonicated for 1 h. The final suspension was transferred in a hydrothermal reactor (250 ml) with heating and continuous stirring at 180 °C for 48 h for unzipping of MWCNTs and sulfonation. After cooling to room temperature, the black suspension was separated, washed with dil. HCl and finally with DI water repeatedly (till neutral pH). The product (sGNR) was dried at 60 °C under vacuum for 12 h.

2.3. Membrane preparation

The nanocomposite membranes of SPEEK/sGNR were prepared by solution casting technique similar to the procedure reported earlier [21]. sGNR in SPEEK with different wt% ratio (viz., 0.05, 0.1 and 0.15) was incorporated. In brief, the required amount of sGNR was sonicated in dimethyl acetamide (DMAc) for 1 h. In parallel, 2 wt% SPEEK was dissolved in DMAc under stirring at room temperature and finally both the solutions were mixed, sonicated and stirred for 4 h. The solution was then poured on a flat glass Petri dish and cast at 80 °C under vacuum for 12 h. The membranes were then peeled-off and the measured thickness varied from 50 to 70 μm.

2.4. Characterization

High resolution transmission electron microscopy (HR-TEM) analysis of MWCNTs and sGNR were performed to study the change in shape and size of sGNR drop cast after dispersing in ethanol on copper TEM grid (TED Pella, Inc., USA) on a Tecnai G2 200 kV FEG TMP, FEI. The surface morphology of pristine SPEEK and its composite membrane SPEEK/sGNR (0.1 wt%) were analyzed in the field emission-scanning electron microscopy (FE-SEM) instrument (Zeiss ultra FE-SEM instruments, Germany), elemental mapping was also done on the same instrument for sGNR to understand the carbon, oxygen and sulfur content distribution. The energy dispersive X-ray spectroscopy (EDS) analysis of MWCNTs and sGNR were analyzed on an EDS detector (quantax) connected to the scanning electron microscopy (SEM) instrument (TESCAN, Vega 3). The atomic force microscopy (AFM) analysis was done for

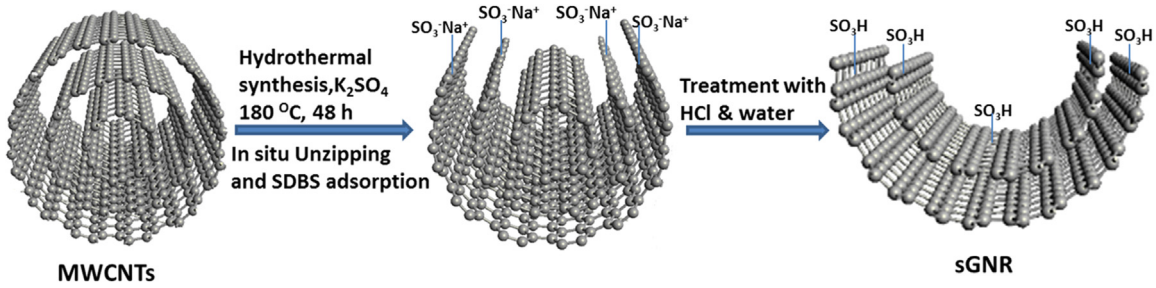

Scheme 1. Mechanism of simultaneous unzipping of multi-walled carbon nanotubes (with the length of 3–6 μm) and adsorption of SDBS to form sulfonated graphene nanoribbons (sGNR).

the MWCNTs, sGNR, pristine SPEEK and its composite membranes in tapping mode atomic force microscopy (AFM, Pico SPM-Picoscan 2100, Molecular Imaging, USA). Raman analysis of MWCNTs and sGNR were performed on HR 800 Raman spectrometer (Jobin Yvon, Horiba, France) using 632.8 nm green laser (NRS 1500 W). The Fourier transform-infrared spectroscopy (FT-IR) of MWCNTs and sGNR were analyzed in a TENSOR 27 (Bruker optik GmbH, Germany). The elemental analysis was done for the MWCNTs and sGNR in Elementarvario EL 111- Germany. The X-ray photoelectron spectroscopy (XPS) analysis was done for MWCNTs and sGNR using Thermo Scientific MULTILAB 2000 Base system with X-Ray, Auger and ISS attachments. The thermo-gravimetric analysis (TGA) was performed on a NETZSCH STA 449F3 TGA-DSC instrument in the nitrogen environment (60 ml min^{-1}) with the heating rate of 5 °C min^{-1} within temperature range of 30 °C and 1100 °C. The mechanical properties in terms of tensile strength and elongation at break of the membrane samples under sorbed condition (dipped in water for 24 h and surface sorbed) was determined using universal testing machine (UTM) (model: ZWICK/Roell, 146500) using ASTMD882 with 10 mm width and 25 mm grip to grip separation of membrane samples. The membrane samples were tested using load cell of 1 kN with the test speed of 2 mm/min. The average of five measurements for each sample was taken into consideration.

2.5. Ion exchange capacity, water uptake, proton conductivity and electrical conductivity

Ion exchange capacity (IEC) was measured using acid-base titration method [19]. The membrane sample with 2 cm^2 area and 60 μm thickness was immersed in a saturated solution of NaCl for 24 h. The membrane was subsequently taken out and the remnant solution was titrated against NaOH solution. IEC is calculated by using the equation given below:

$$IEC = \frac{V_{NaOH} \times N_{NaOH}}{Dry\ \ weight\ \ of\ \ sample}\ \text{meq g}^{-1} \tag{1}$$

where V_{NaOH} and N_{NaOH} represents the volume of NaOH consumed during the titration and concentration of NaOH (in normality) used for the titration.

The water uptake was measured by subjecting 2 cm^2 area of the dried membranes free of moisture kept in DI water for equilibration at room temperature for 24 h [22]. The membrane was then surface sorbed and finally weighed. The water uptake was calculated by the difference in the weight of the sorbed and dry membranes from the equation given below:

$$Water\ \ uptake(\%) = \left[\frac{W_{eq.} - W_{intial}}{W_{intial}}\right] \times 100 \tag{2}$$

where $W_{eq.}$ and $W_{initial}$ represent the weight of the equilibrated and initially dried membrane respectively.

The proton conductivity of the membrane was measured in a fuel cell mode set-up by subjecting the membrane electrode assembly to an alternating voltage signal of rms value 10 mV in the frequency range of 1 MHz to 100 mHz. The impedance of the membranes was measured at different temperatures ranging from the room temperature to 60 °C under the fully humidified condition at 0.6 V (nearing Ohmic region). The Ohmic resistance was noted by high frequency intercept of impedance with the real axis. Finally ionic conductivity was calculated using the relation given below:

$$Membrane\ \ specific\ \ conductance = \frac{Thickness\ \ of\ \ membrane}{Area\ \ specific\ \ resistance}\left(\text{S cm}^{-1}\right) \tag{3}$$

The setup for measuring electrical conductivity i.e. conductivity cell arrangement consisting of two stainless steel electrodes of 20 mm diameter each was arranged in a Teflon set-up. The completely dried membrane at 80 °C for 24 h was placed in between the two electrodes and the set-up was kept in a closed glass container. The setup was heated at 60 °C to remove the moisture and also to reach the fuel cell operation temperature. Autolab PGSTAT 30 instrument was used for the measurement of AC impedance with amplitude of 10 mV in the frequency range of 1 MHz to 1 Hz for different membrane samples. The high frequency intercept on real axis of the impedance spectrum was used to determine the resistance (R) of different membrane samples. The electrical conductivity of the membrane samples was determined by the equation:

$$\sigma = \frac{l}{RA} \tag{4}$$

where σ represents the electrical conductivity of the membrane samples in S/cm, l stand for the thickness of membrane sample in cm, R stands for the electrical resistance of membrane and A stands for cross-sectional area of membrane in cm^2.

2.6. Fabrication of membrane electrode assembly (MEA)

MEAs were fabricated similar to the procedure reported elsewhere [23]. In brief, the catalyst slurry was prepared using 40 wt% platinum supported on carbon with iso-propyl alcohol as a solvent and Nafion solution (5 wt%) as a binder. The electrodes were further prepared by loading the above with 0.5 mg cm^{-2} catalyst layer brush coated on the commercial gas diffusion layer. Further the aforesaid composite membrane was uni-axially sandwiched between the electrodes and hot pressed (hydraulic press) at 80 °C with a compaction load of 20 kg cm^{-2} for 2.5 min to form MEA.

2.7. Fuel cell performance evaluation

MEAs were assembled in a single cell of 25 cm^2 active area

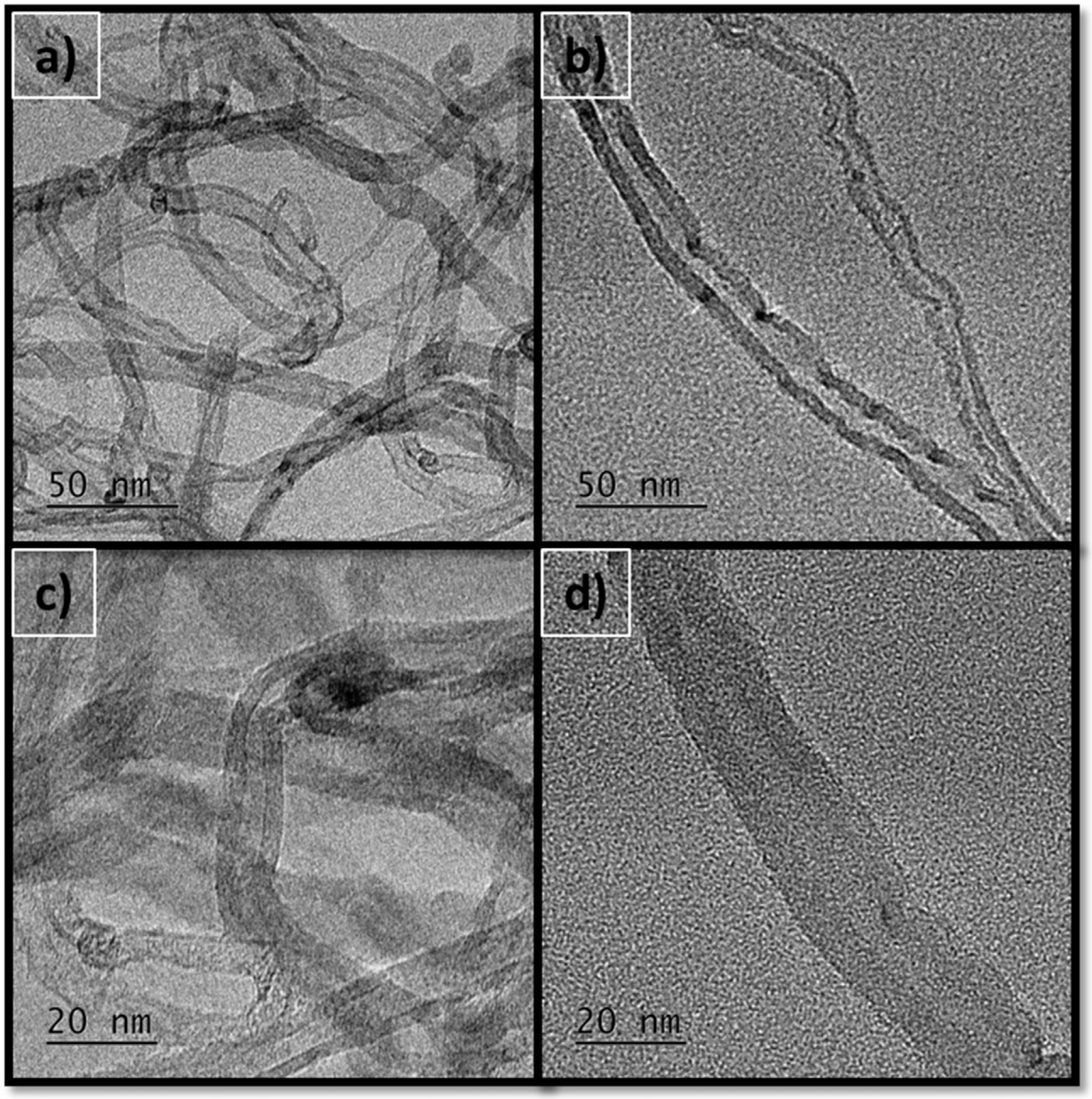

Fig. 1. HR-TEM images of pristine MWCNTs (a and c) and sGNR (b and d). Unzipping of pristine MWCNTs is seen with the increase in the width from 5–10 nm to 15–20 nm with the smooth edges and few transparent layers of sGNR. Length scale (a,b) is 50 nm and of (c & d) is 20 nm.

comprising graphite monopolar plates with serpentine flow field along with current collector and end plates supplied by Fuel Cell Technologies, Inc., USA. The cell was further stabilized/activated at 0.6 V to observe the steady state current and then tested for polarization (I-V characteristics). High purity H_2 and O_2 with the stoichiometry of 1.2 and 3 were fed as a fuel and oxidant on anode and cathode side for PEMFC test respectively. Galvanostatic polarization experiments were carried out at 60 °C after stabilizing the fuel cell under fully humidified conditions (100% RH) on both sides in an electronic load Model: LCN1-50-24 and LCN1-100-24 from Bitrode Instrument (Bitrode Corp. Fenton MO USA).

2.8. Accelerated durability test (ADT)

The accelerated durability test (ADT) was performed for the pristine SPEEK and its optimized nanocomposite membrane SPEEK/sGNR (0.1 wt%) for 100 h and also the ADT was extended for the composite membrane up to 200 h to evaluate the further degradation point. DOE (US) protocols were slightly modified suiting to the characteristics of SPEEK matrix and its composite stability. The ADT measurement was performed in OCV condition at 60 °C cell temperature and at 30% RH on both the anode and cathode side with the fuel flow rate of hydrogen 350 ml min^{-1} on anode side and 870 ml min^{-1} of air on cathode side. The test was performed in an electronic load Model: LCN1-100-24 from Bitrode Instrument (Bitrode Corp. Fenton MO USA). After every 25 h of test, the cell was subjected to the gas permeability measurement (H_2 cross-over) and electrochemical impedance spectroscopy (EIS) to understand the degradation behavior during durability test.

The gas permeability (H_2 fuel cross-over) measurement was performed in potentiostat/galvanostat (Autolab PGSTAT 30) instrument in the fuel cell set-up by linear sweep voltammetry (LSV). The working electrode was connected on cathode side and the counter and reference electrode was connected on anode side of the fuel cell set-up. The humidified H_2 gas was passed on anode side with flow rate of 350 ml min^{-1} and humidified N_2 gas was passed on the cathode side with the flow rate of 150 ml min^{-1}. The LSV measurement after equilibrating the cell for 1 h was

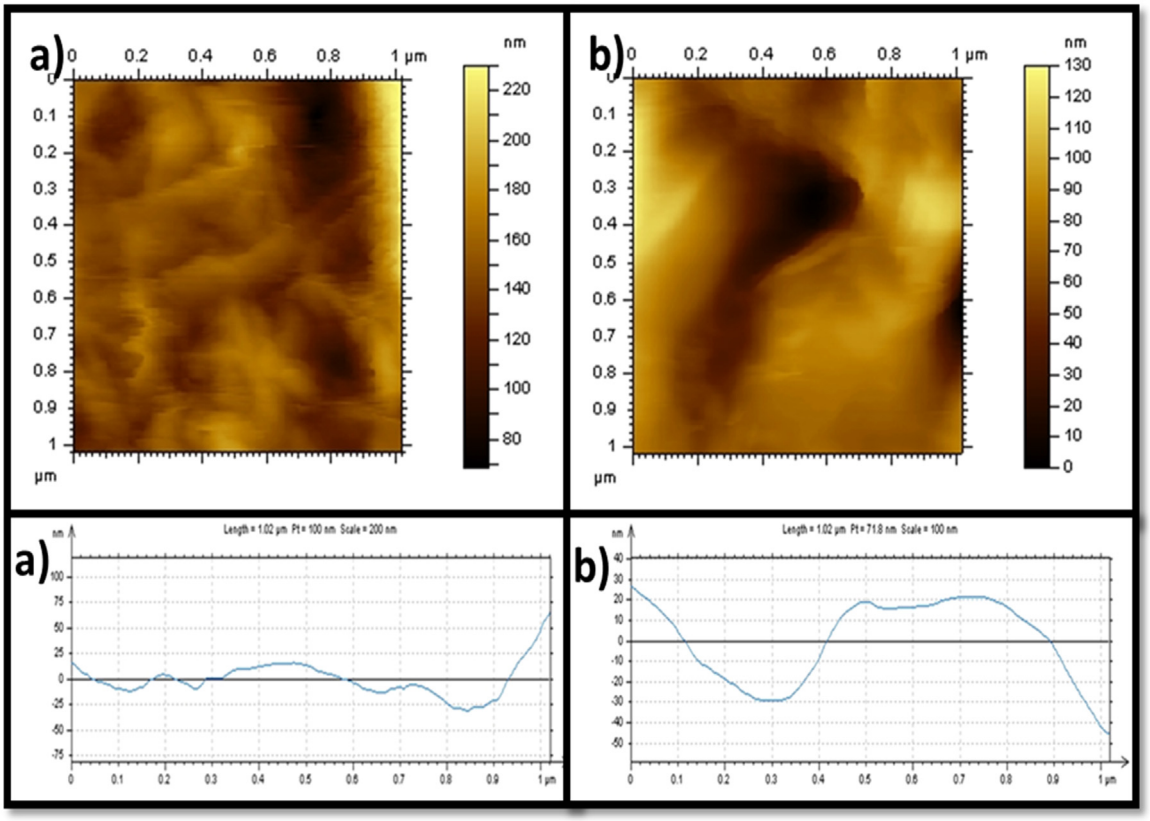

Fig. 2. AFM analysis of (a) MWCNTs and (b) sGNR. The decrease in the height of the GNRs (9.85 nm) (including SDBS adsorption on both the sides) compared to the pristine MWCNTs (15 nm) shows some of the layers are successfully exfoliated to sGNR with smooth edges.

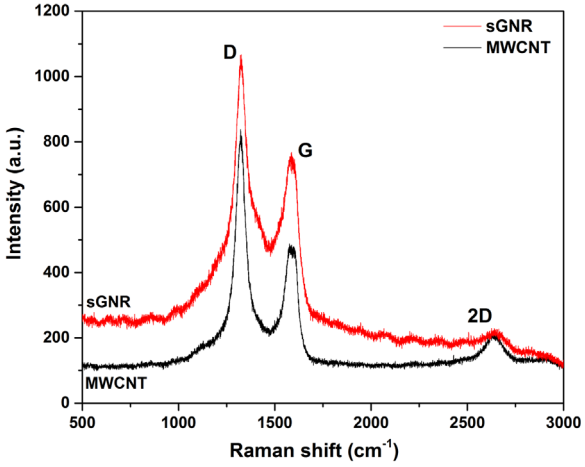

Fig. 3. Laser-Raman spectra of MWCNTs and sGNR. Lower I_D/I_G ratio (1.38) for sGNR is observed compared to pristine MWCNTs (1.70) suggesting towards the low defect density. I_{2D}/I_G ratio of 0.30 suggests 3–5 layers of sGNR present.

performed with the scan rate of 5 mV s^{-1} between 0.05 and 0.4 V at room temperature (~25 °C) to measure the H_2 cross-over current from anode to the cathode side, which is electrochemically oxidized on cathode side.

The electrochemical impedance spectroscopy (EIS) measurements for the pristine SPEEK and SPEEK/sGNR (0.1 wt%) nanocomposite membrane was performed on fuel cell test station (Biologic, Model: FCT-150S) after every 25 h of ADT. The test was carried out with H_2 as anode side fuel and O_2 as cathode side oxidant under fully humidified condition at operating temperature of 60 °C. The reactant gas stoichiometry of 1.2 and 3 for H_2 and O_2 respectively, at ambient pressure was maintained. The EIS measurements were carried out at 0.8 V.

3. Results and discussion

3.1. Structural characterization of MWCNTs and sGNR

Previous studies clearly indicate the important role of defects in MWCNTs as a primary cause for the longitudinal unzipping to GNR especially in presence of the electric field. Increased defects in MWCNTs can be created by aggressive chemical reagents like K_2SO_4 in aqueous medium and further intercalation of potassium and sulfate ions through these defects on the edge and grain boundaries will exfoliate the MWCNT and expand the interlayer distance of MWCNT which will then facilitate the longitudinal unzipping of MWCNT to form GNR at hydrothermal conditions of temperature and pressure [20]. In situ hydrothermal synthesis route is followed for simultaneous unzipping of MWCNT and adsorption of SDBS. SDBS is adsorbed in the GNR due to the weak π-π and hydrophobic interactions between them to form sulfonic acid group functionalized GNR (sGNR) [18]. It is also presumed that Na^+ ion (from SDBS) being smaller in size compared to K^+ also intercalate inside the pristine MWCNT layers which can enhance the unzipping to form GNR. Accordingly a probable structural modification of MWCNTs during this reaction is represented in Scheme 1.

HR-TEM (Fig. 1b and d) images interestingly show the unzipping in MWCNTs along with an increase in the width compared to that of pristine MWCNTs (Fig. 1a and c) from 5–10 nm to 15–20 nm with smooth edges. More importantly few transparent layers of sGNR can also be discerned in these images. It confirms the unzipping of MWCNTs despite in a smaller degree which provides valuable clue for the possible interaction between sulfonated GNR

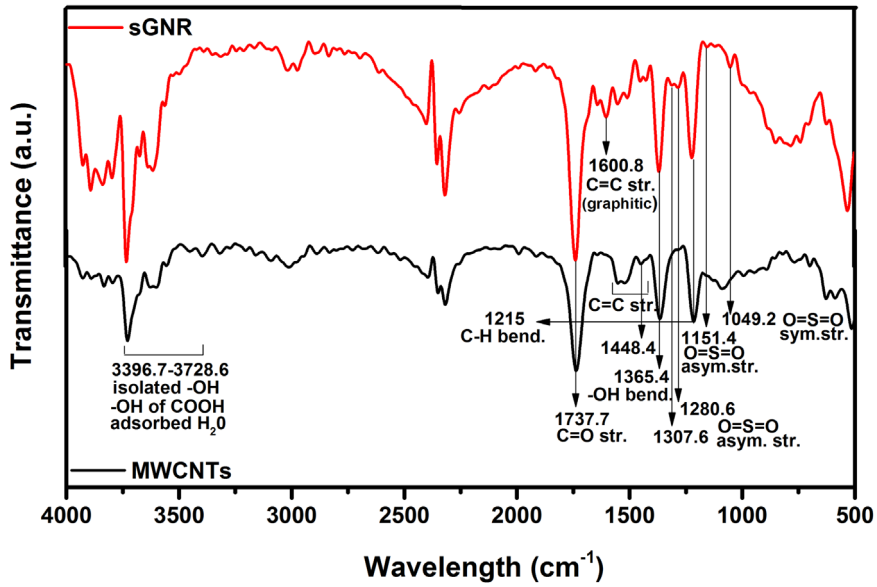

Fig. 4. FT-IR spectra of MWCNTs and sGNR. Adsorption of SDBS on the GNR and also conversion of MWCNTs to the sGNR with the graphitic peak is confirmed.

and sulfonated MWCNT [24].

The AFM analysis was performed to know the more accurate shape and size of sGNR. The unzipped product shows a significant decrease in the height (9.85 nm including SDBS on both sides of GNR) as compared to that of MWCNTs with the height of 15 nm confirming the unzipping of MWCNTs up to few layers as seen in Fig. 2. The AFM of sGNR also show long ribbons (2–3 μm) with smooth edges.

Raman spectroscopy is used to determine the changes in the important characteristics of carbon nanotubes during its transformation to GNRs. Since the I_D/I_G ratio is an important parameter to determine the defect density, disorder, edge smoothness [25] and edge structures [26–28]. As shown in Fig. 3, the I_D/I_G ratio of sGNR is 1.38 which is comparatively lower than 1.70 for pristine MWCNTs, suggesting towards the low defect density. The slight broadening and consequent shift in the position of G band is due to the disordered structure of sGNR because of the subtle morphology changes after unzipping in comparison to that of pristine MWCNTs [20]. More significantly a finite change in the I_{2D}/I_G ratio, being π electron sensitive (suggesting the layer thickness) from 0.30 to 0.45 for pristine MWCNTs suggests the presence of about 3–5 layer of sGNR which is an indication of unzipping [20].

FT-IR analysis has been carried out to confirm the chemical changes after sulfonation and accordingly, Fig. 4, shows a comparison of the IR spectra of the MWCNTs before and after the hydrothermal treatment. Pristine MWCNT spectrum shows the C=C stretching frequency of MWCNTs at 1448.4 cm^{-1} and in the range of 1444.5–1552.6 cm^{-1} [11,29] while peaks in the range of 3396.7–3728.6 cm^{-1} correspond to the stretching vibrations of isolated O-H group/O-H group of carboxylic acid and adsorbed water respectively [30]. The peak at 1737 cm^{-1} represents the C=O of carboxylic group and peak at 1365.4 cm^{-1} represents the bending vibration of O-H of carboxylic group [11]. The peak at 1126.3 cm^{-1} represents the C-O stretching frequency of ethers and alcohols [11]. The peak at 1215 cm^{-1} represents the bending vibration of C-H for the benzene ring [11]. There are new prominent peaks in sGNR in comparison to that of the pristine MWCNTs like the one at 1600 cm^{-1} representing the graphitic C=C stretching vibration [31]. Absorption peaks at 1049.2 cm^{-1} and 1151.4 cm^{-1} represent the symmetric and asymmetric stretching vibrations respectively for O=S=O of sulfonic acid group in sGNR compared to that of pristine MWCNTs [11,32,33] while peaks at 1280.6 cm^{-1} and 1307.6 cm^{-1} may be attributed to the asymmetric stretching vibrations of O=S=O sulfonic acid group attached to the untreated sGNR.

XPS is an important surface analytical technique used to measure the elemental composition, chemical valence of the attached functional groups and also the structural defects on the nanotube surface [11,34,35]. The XPS analysis survey spectra of pristine MWCNTs, sGNR and its deconvoluted spectra are shown in Fig. 5. In pristine MWCNTs, carbon and oxygen are present in C1s and O1s state whereas in sGNR, additional S2p state of sulfur confirms the presence of sulfonic acid group as seen in Fig. 5a (survey spectra). The deconvoluted spectrum for the C1s in Fig. 5b of pristine MWCNTs shows different peaks for C=C (284.89 eV); C–O (286.17 eV); C–O (287.29 eV) [11] signals and also a π-π* transition loss peak (291.20 eV) [34]. Further the deconvoluted spectrum of O1s in pristine MWCNTs (Fig. 5d) shows different peaks for C=O (532.87 eV) [11]; C–O–C, C-O-H (533.87 eV) [11] and isolated –OH, C=O, and finally O-C=O (531.61 eV) [34]. In comparison, the deconvoluted XP spectrum for C1s for sGNR in Fig. 5c shows different peaks for C=C (284.64 eV)[11]; C-C, C-H [11], defects in nanotube structure (285.52 eV) [34]; C-O (286.53 eV) [11,34] and C=O (287.32 eV). [11,36] Similarly the deconvoluted spectrum for O1s in sGNR shown in Fig. 5e confirms the presence of peaks for C=O (532.60 eV) [11,34]; C-O-C, C-O-H, S=O (533.94 eV) [11,34]. Finally, the deconvoluted XP spectrum of S2p for sGNR in Fig. 5f shows peaks at S2p1/2 (169.65 eV) and S2p3/2 (168.75 eV) with a separation of 0.9 eV, which confirms the presence of sulfonic acid groups [11,37] although the reasons for diminished S2p peak intensity for sGNR could be attributed to the less number of sulfur atom present in the SDBS molecule [37].

Thermogravimetric analysis (TGA) of both pristine MWCNTs and sGNR are shown in Fig. S1 of the Supplementary material. The TGA curve of pristine MWCNTs shows a weight loss starting at 875 °C due to the decomposition of MWCNTs [34,38] while in sGNR, the first weight loss of 7.2 wt% is in the range of 305.7–500.5 °C due to the decomposition of the functional groups/sulfonic acid groups attached to the GNR [34,39]. The residue obtained at 1162.8 °C was 59.7% in the pristine MWCNTs while it is only 34.8% in the sGNR explaining the contribution from the modification of MWCNTs.

The CHNS analysis of MWCNTs and sGNR was performed and the content of specific elements present in it is shown in Table S1

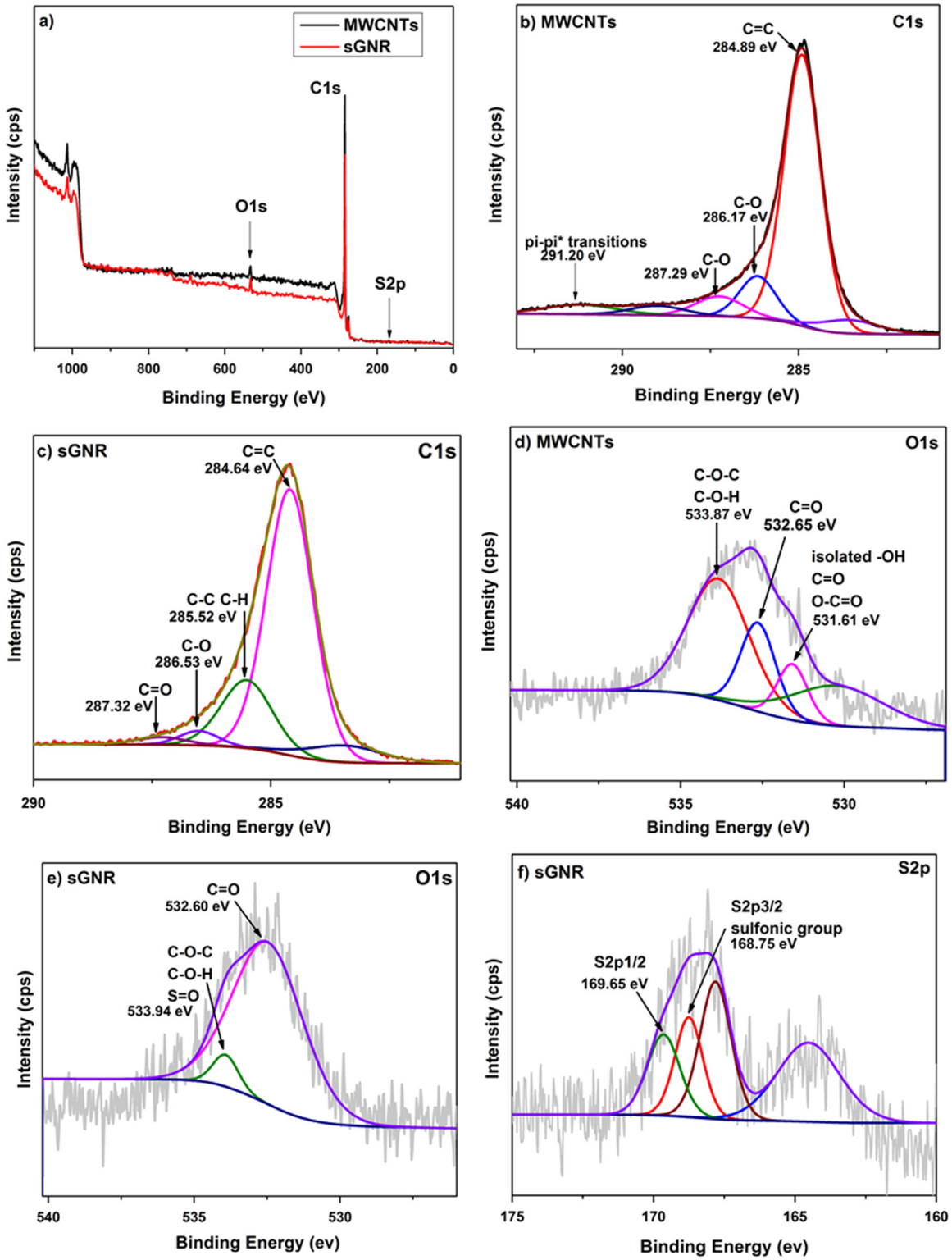

Fig. 5. XPS analysis (a) survey spectra for MWCNTs and sGNR, (b and c) C1s deconvoluted spectra for MWCNTs and sGNR, (d and e) O1s deconvoluted spectra for MWCNTs and sGNR and (f) S2p deconvoluted spectrum for sGNR, confirming the presence of sulfonic acid group along with the different functional moieties in sGNR.

of the Supplementary material. The sulfur and hydrogen content of 2.8% and 1.4% observed for sGNR confirms sulfonation. Interestingly, the degree of sulfonation calculated from CHNS is found to be 3% by considering the sulfur and carbon content [40] which are in correlation with 7.2 wt% of the sulfonic acid group loss in TGA. Further increase of oxygen and sulfur content in sGNR compared to that of MWCNT as observed in Table S2 (see Supplementary material) derived from EDS spectra suggests the attachment of $-SO_3H$ group to GNR perhaps at the edges. The elemental mapping of sGNR shown in Fig. S2 (see Supplementary material) also confirms the uniform distribution of carbon, oxygen and sulfur providing further credibility to above degree of sulfonation.

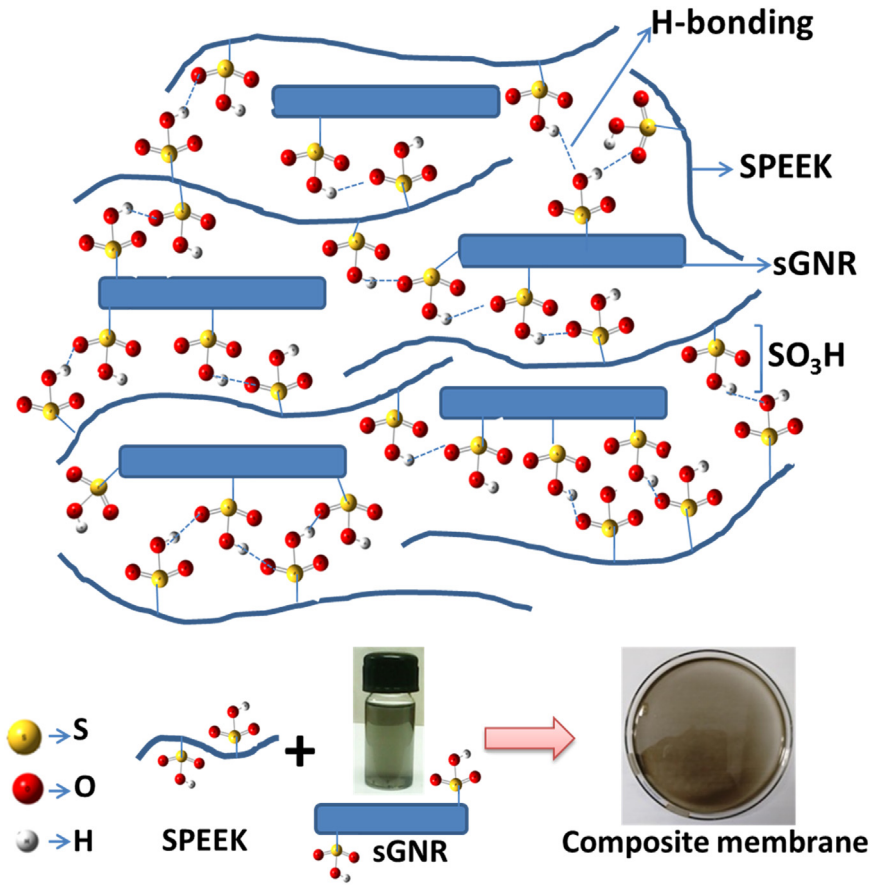

Scheme 2. Hydrogen bonding interaction of sulfonated graphene nano-ribbons and sulfonated polyether ether ketone to form nanocomposite membranes. The sGNR dispersion in to the SPEEK matrix is uniform as seen in the photograph.

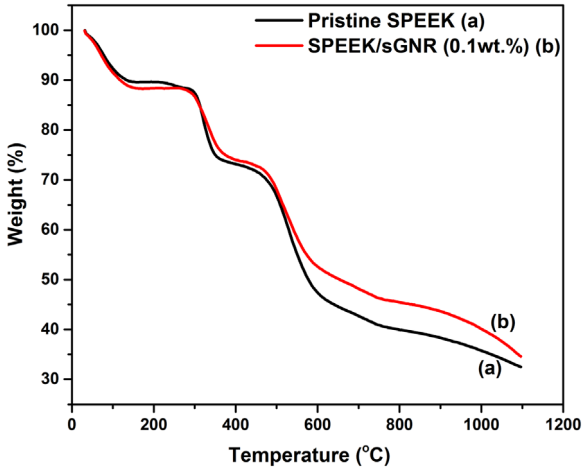

Fig. 6. TGA of (a) pristine SPEEK and (b) SPEEK/sGNR (0.1 wt%). It represents that the composite membrane have similar thermal stability as pristine SPEEK.

3.2. Characterization of pristine SPEEK and composite membranes

Based on the combined experimental data presented above, it is possible to understand the probable interaction between sGNR and SPEEK as illustrated in Scheme 2 (along with photographs of the dispersed sGNR and SPEEK/sGNR composite membrane). Thermo-gravimetric analysis (TGA) of pristine SPEEK and SPEEK/sGNR (0.1 wt%) composite membranes show support for this scheme in the form of three regions of thermal degradation as represented in Fig. 6. The first thermal degradation region lies in the range of 50–130 °C which is mainly due to the adsorbed moisture in the membrane. The second region between 290 and 380 °C is perhaps due to the degradation of the sulfonic acid group while the third region in between 450 and 630 °C could be ascribed to the degradation of the main polymeric chain [19].

A comparison of the surface morphology of pristine SPEEK and SPEEK/sGNR is represented in Fig. 7, where the composite membranes show enhanced surface roughness in comparison with the smooth morphology for the pristine SPEEK confirming the uniform dispersion of sGNR in SPEEK matrix. No agglomeration or phase separation of particle is found and further neither cracks nor defects is evident for these membranes which is also in accordance with the literature available for such composite membranes [18]. FE-SEM cross-sectional analysis for the same also confirms the distribution of sGNR in pristine SPEEK as seen in Fig. S3 of the Supplementary material. Pristine SPEEK however, shows smooth morphology even in magnified plane (Fig. S3b) whereas SPEEK/sGNR (0.1 wt%) composite membrane in the magnified plane (Fig. S3d) shows only the distribution of sGNR in SPEEK. This may facilitate enhanced transport of protons during PEFC operation.

The surface topography changes for the pristine SPEEK as well as SPEEK/sGNR (0.1 wt%) composite can be understood by comparing the AFM images as represented in Fig. 8. For example, brighter regions seen in SPEEK/sGNR (0.1 wt%) composite membrane (Fig. 8b and d) suggests the preponderance of hydrophilic, sulfonic acid groups of sGNR interacting with the hydrophilic domains of SPEEK (Fig. 8a and c) [41,42]. Composite SPEEK/sGNR (0.1 wt%) membrane also shows uniform distribution of sGNR additives in the base polymer SPEEK. The increment in the hydrophilic sulfonic acid groups is due to the presence of sGNR additive in the sulfonated chain of PEEK matrix. The increase in the

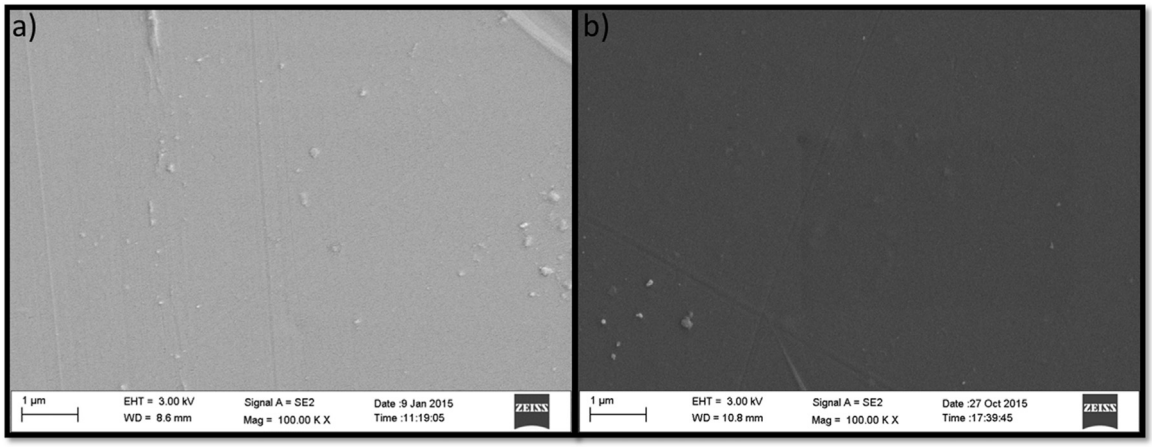

Fig. 7. FE-SEM surface morphologies for (a) pristine SPEEK and (b) SPEEK/sGNR (0.1 wt%). Uniform distribution of sGNR in SPEEK is observed.

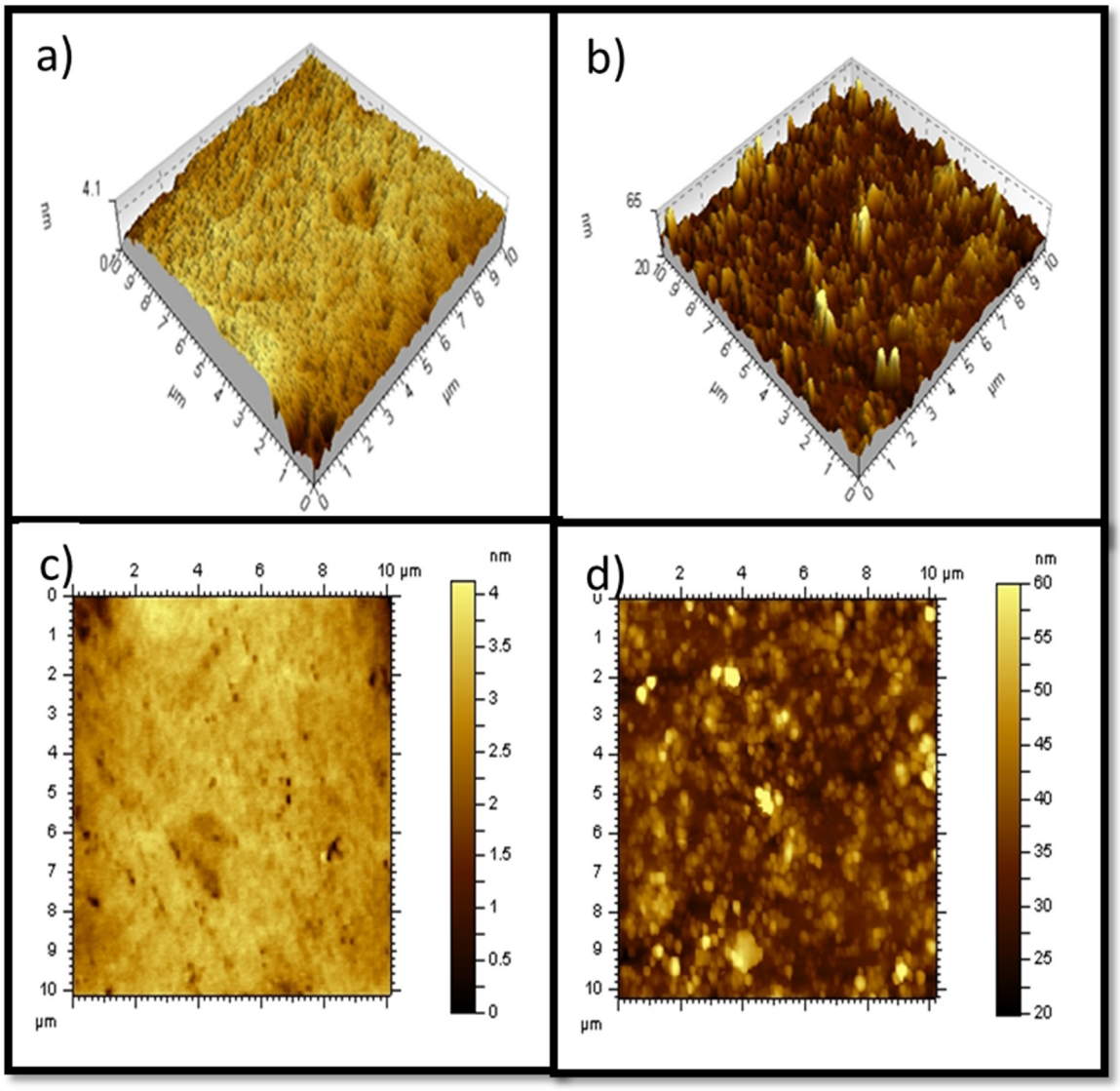

Fig. 8. AFM analysis of (a and c) Pristine SPEEK and (b and d) SPEEK/sGNR (0.1 wt%). Brighter regions seen in composite membrane suggests the hydrophilic sulfonic acid groups of sGNR interacting with the hydrophilic domains of SPEEK.

hydrophilic sulfonic acid groups in the composite membrane is perhaps, responsible for the more energetically favorable path for proton transport due to functional compatibility from the dual hydrophilic domains.

The mechanical properties in terms of tensile strength and elongation at break for different membranes are represented in

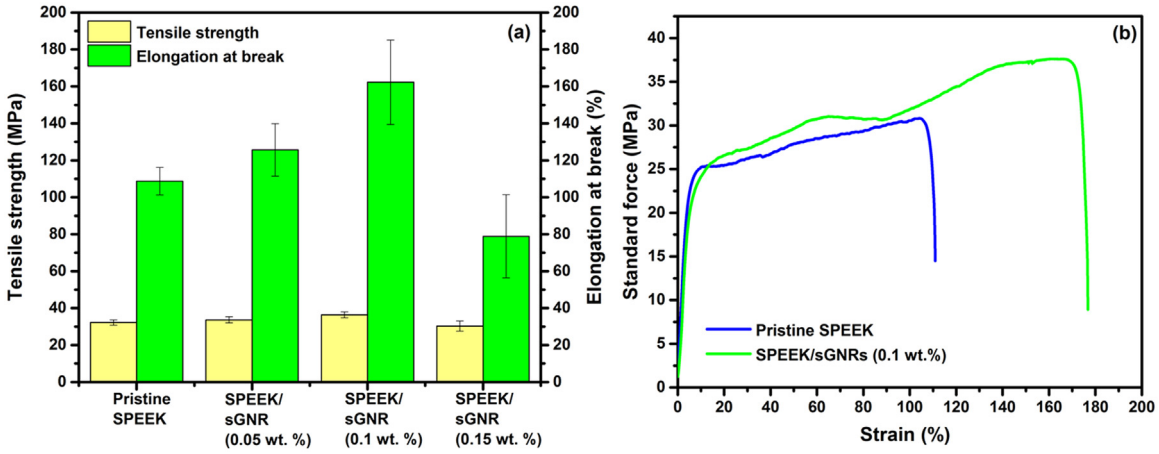

Fig. 9. (a) Tensile strength and elongation at break under sorbed condition for pristine SPEEK and nanocomposite membranes. (b) Stress-Strain curve for pristine SPEEK and SPEEK/sGNR (0.1 wt%) composite membranes suggesting the better mechanical strength for 0.1 wt% sGNR additive in SPEEK matrix.

Table 1
IEC, water uptake, proton conductivity, activation energy of proton conduction (Ea), and Area specific resistance in cell mode of the Pristine SPEEK, and sGNR-incorporated SPEEK (SPEEK/sGNR) Membranes.

Membrane type	IEC (meq g^{-1})	Water uptake (%)	Proton conductivity for membranes		Activation energy E_a (kJ mol^{-1})	Area specific resistance of the membranes ($\times 10^{-7}$ Ω cm^2)
			33 °C (mS cm^{-1})	60 °C (mS cm^{-1})		
Pristine SPEEK	0.78	28.81	36.32	53.63	11.14	5.33
SPEEK/sGNR (0.05 wt%)	1.54	40.48	39.25	57.97	10.81	3.93
SPEEK/sGNR (0.1 wt%)	1.42	37.35	43.81	63.45	10.56	2.36
SPEEK/sGNR (0.15 wt%)	1.41	36.75	24.99	44.39	15.88	6.12
Nafion 212	0.31	22.77	52.94	76.34	9.89	1.60

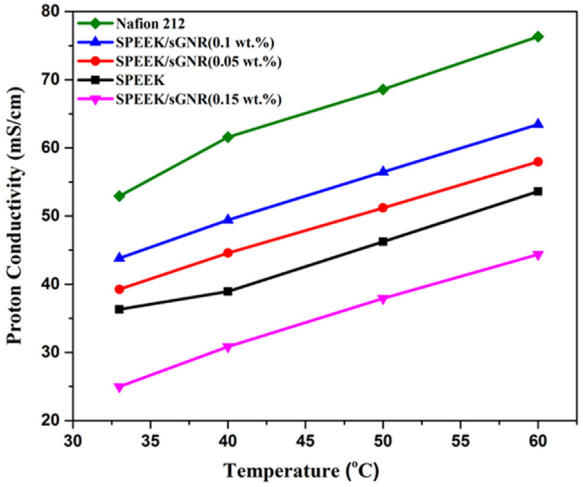

Fig. 10. Proton conductivity of SPEEK, SPEEK/sGNR composite membrane and Nafion 212. The proton conductivity of composite membrane has increased compared to the pristine SPEEK and SPEEK/sGNR (0.1 wt%) has shown the highest conductivity among all the composite membranes. Nafion 212 has better conductivity than other composite membranes.

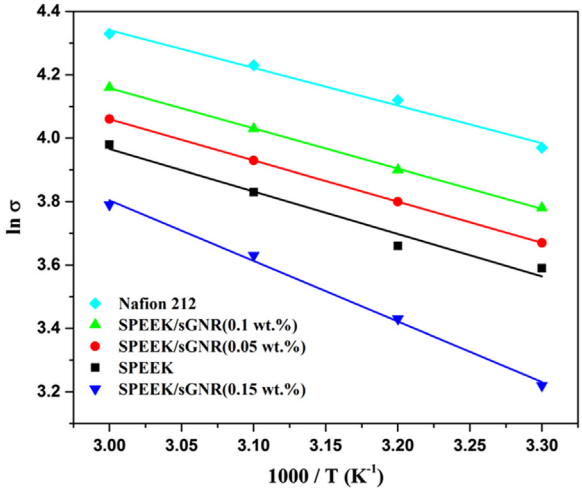

Fig. 11. Arrhenius plot for SPEEK, SPEEK/sGNR composite membrane and Nafion 212. The lower activation energy for ionic transport is observed for the SPEEK/sGNR (0.1 wt%) compared to the pristine SPEEK and other composites.

Fig. 9a. The tensile strength and elongation at break of SPEEK/sGNR (0.05 wt%) nanocomposite membrane increased compared to pristine SPEEK due to the addition of sGNR as additive which impacts the mechanical properties of the composite membrane. Moreover, the SPEEK/sGNR (0.1 wt%) nanocomposite membrane show better tensile strength as well as elongation at break compared to pristine SPEEK and SPEEK/sGNR (0.05 wt%) due to the presence of GNR in significant amount with excellent mechanical strength [20] and uniform distribution in SPEEK, which may strengthen the SPEEK polymer chains. Further as the addition of sGNR increased to 0.15 wt% in the composite membrane, the tensile strength and elongation at break reduced compared to the SPEEK/sGNR (0.1 wt%) and pristine SPEEK, may be due to the agglomeration of sGNR particles which disturbs the chain continuity of pristine SPEEK due to the higher content of additive [43]. Stress-strain curve for pristine SPEEK, SPEEK/sGNR (0.1 wt%) is also represented in Fig. 9b, which shows higher mechanical stability of the optimized composite membrane compared to pristine matrix. The statistical significance analysis is calculated and is found that the tensile strength and elongation at break for all the four membrane samples represented in Fig. 9a has the p-value of 0.0058 and 0.0013 respectively, which is lesser than the

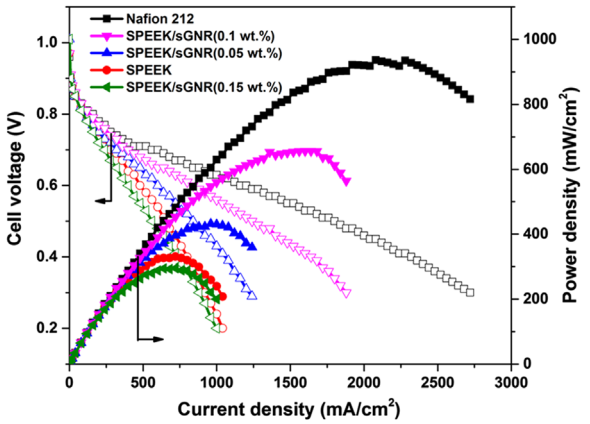

Fig. 12. Cell polarization for the MEAs in PEMFCs. The current density of 840 mA cm^{-2} is observed at 0.6 V (peak power density of 660 mW cm^{-2}) for SPEEK/sGNR (0.1 wt%) compared to the pristine SPEEK of 480 mA cm^{-2} at 0.6 V (peak power density of 331 mW cm^{-2}).

significance level (α) of 5% (0.05), confirms the statistical significance between four sample groups for the above properties.

3.3. IEC, water uptake and proton conductivity for the membranes

For a PEMFC application, IEC, water uptake and proton conductivity provide some vital parameters interconnected to each other which in turn determines the overall fuel cell performance. Ion exchange capacity (IEC) suggests the ability of membrane to exchange the protons with the ions of solution in contact. The IEC of the composite membranes of SPEEK/sGNR increases in comparison to pristine SPEEK due to the increased amount of sulfonic acid groups in the composite membranes as shown in Table 1. The water uptake for the aforesaid composite membranes also increases in comparison to the pristine SPEEK as shown in Table 1 due to the increased content of hydrophilic sulfonic acid group in the composite membrane. This in turn is expected to facilitate more water molecules getting absorbed almost reaching a steady state saturation at different content of sGNR. Interestingly, the proton conductivity of composite membranes with sGNR content of 0.05 wt% and 0.1 wt% also increases compared to that of pristine SPEEK suggesting enhanced ionic conducting paths of SPEEK both at 30 °C and 60 °C at 100% RH with the dispersion of sGNR. The hydrophilic sulfonic acid group is responsible for improved water uptake which in turn facilitates the proton conductivity. At the same time the additional sulfonic acid groups through sGNR in the composite membrane also facilitate proton transfer by contributing more towards the available sites for ionic transport. However when the content is above 0.1 wt%, it was presumed that the paths may be disturbed extensively by electrical conductivity thereby reducing proton transport. To further confirm the same, the electrical conductivity of pristine SPEEK and its composites were studied to understand the effect of high electrically conducting additive, i.e. sulfonated GNR in pristine SPEEK. The average of five values was considered as a measure of final electrical conductivity. As seen in the Fig. S4 of the Supplementary material, the electrical conductivity of pristine SPEEK and its composites are approximately in the same range and as the additive (sGNR) content in the composite membranes is very less i.e. lesser than the percolation threshold (2 wt%) [14], there is a negligible effect on the electrical conductivity of composite membranes. So it is confirmed that the reduced ionic conductivity is attributed to the agglomeration of sGNR (0.15 wt%) obstructing proton transport due to its high content in the SPEEK matrix [43]. It is important to note that IEC and water uptake is higher for pristine SPEEK and nanocomposite membranes of SPEEK/sGNR when compared to Nafion 212 due to the higher degree of sulfonation. However proton conductivity of SPEEK and its composites is lesser in comparison to Nafion 212 due to the lower hydrophilic/hydrophobic separation corresponding to narrow channels in the network [44].

3.4. Activation energy for proton conduction

The activation energy for proton transport (the minimum energy required for the ionic transport in the membrane) in pristine SPEEK and composite membranes is determined by measuring proton conductivity at different temperature as displayed in Fig. 10. The activation energy E_a (kJ mol^{-1}) can be calculated by the Arrhenius equation given below through a linear fit [18,45] of Fig. 11.

$$\ln\sigma = \ln\sigma_0 - \frac{E_a}{RT} \quad (4)$$

where σ is the proton conductivity (mS cm^{-1}), σ_o is the pre-exponential factor (mS cm^{-1}), R is the gas constant and T is the temperature (K). As shown in Table 1, the activation energy is less for the composite membrane with sGNR content of 0.05 wt% and 0.1 wt% suggesting enhanced ionic transport through the membrane in comparison to SPEEK. However if the content is above 0.1 wt%, the activation energy is higher suggesting more energy required to transport the protons through the composite membrane (0.15 wt%), may be due to the blockage of ionic channels of SPEEK because of agglomeration of sGNR at higher additive concentration [43].

3.5. Steady state polarization

The aforesaid SPEEK/sGNR composite membrane based MEAs are subjected to cell polarization using humidified H_2 and O_2 as fuel and oxidant respectively at ambient pressure. The experimental data are also compared with the data obtained using pristine SPEEK and Nafion 212 based MEAs as represented in Fig. 12. Interestingly, the composite membranes with 0.05 and 0.1 wt% content of sGNR show better peak power density than the pristine SPEEK due to higher proton transport along with enhanced water uptake and IEC. It is obvious that there is an improvement in the Ohmic region for the composite membranes compared to that of pristine SPEEK and at the same time all the curves show similar trend in the activation region indicating same electro catalytic behavior during testing. Also the area specific resistance (ASR) for all the membranes in the region of 0.7–0.5 V for MEAs in fuel cell assembly was calculated and represented in Table 1. ASR significantly decreases for SPEEK/sGNR (0.05 wt% and 0.1 wt%) in the test cell assembly compared to that using pristine SPEEK suggesting improved proton conduction in composites, leading to an improvement in the overall cell performance. However there is also an increased resistance for the composite membrane with the content of 0.15 wt% sGNR due to its agglomeration in the matrix as discussed elsewhere. The SPEEK/sGNR (0.1 wt%) composite has shown better performance (660 mW cm^{-2}) followed by SPEEK/sGNR (0.05 wt%) (432 mW cm^{-2}) in comparison to pristine SPEEK (331 mW cm^{-2}) at 60 °C. However, Nafion 212 has shown better fuel cell performance than all the membranes due its higher proton conductivity.

3.6. Accelerated durability test (ADT) for the membranes

The accelerated durability test (ADT) was performed for the pristine SPEEK and its optimized SPEEK/sGNR (0.1 wt%) nanocomposite membrane. From Fig. 13a, it is observed that the pristine SPEEK membrane has open circuit voltage (OCV) of 0.99 V and after 35 h, it is reduced to 0.9 V and after that sharp fall in OCV is

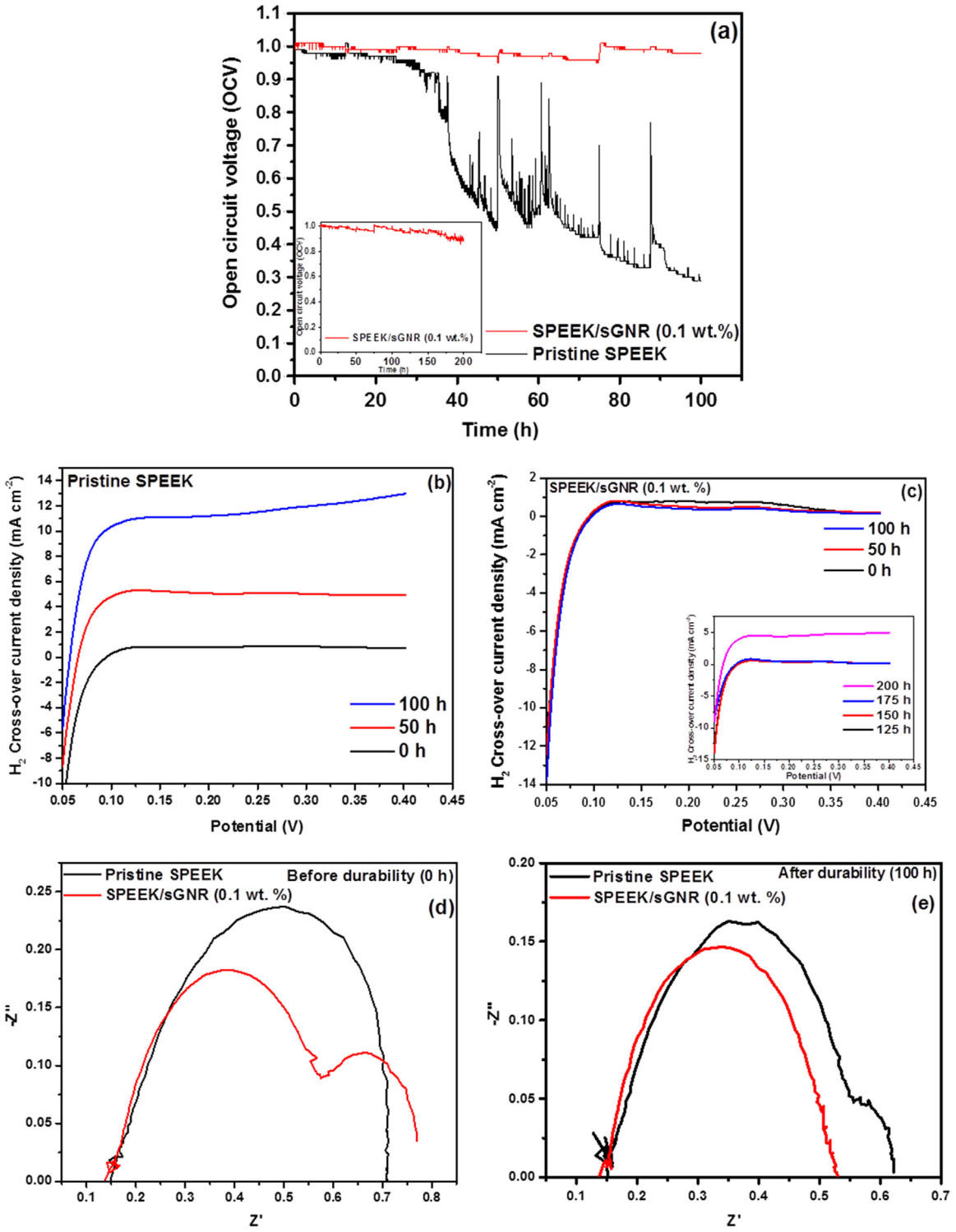

Fig. 13. Accelerated durability test (ADT) curve for (a) pristine SPEEK and SPEEK/sGNR (0.1 wt%) nanocomposite membranes. The ADT of composite membrane up to 200 h is also shown in inset. The hydrogen cross-over curve of (b) Pristine SPEEK for 0, 50 and 100 h during durability and (c) SPEEK/sGNR (0.1 wt%) composite membrane for 0, 50 and 100 h and in inset up to 200 h during durability. The electrochemical impedance spectroscopy (EIS) of pristine SPEEK and SPEEK/sGNR (0.1 wt%) nanocomposite membrane (d) before durability (0 h) and (e) after durability (100 h).

seen till 0.8 V and after 100 h it is 0.29 V which is 70% degradation of initial OCV. Whereas in SPEEK/sGNR (0.1 wt%) nanocomposite membrane ADT, the initial OCV observed was 1.01 V and there is no sharp degradation in OCV up to 100 h. The OCV of 0.98 V was observed after 100 h which is only 3% degradation of initial OCV. To observe the sharp degradation point in the nanocomposite membrane, the ADT was further continued up to the 200 h and the final OCV observed was 0.9 V which is only 11% degradation in voltage of initial OCV (inset to Fig. 13a). So the durability of the optimized SPEEK/sGNR (0.1 wt%) nanocomposite membrane in relation to initial OCV is on the higher side in comparison to the pristine SPEEK. The reason for higher durability of the SPEEK/sGNR (0.1 wt%) nanocomposite membrane in comparison to the pristine SPEEK is due to the presence of highly stable additive i.e. sGNR

with excellent mechanical and thermal properties [20] with uniform distribution in SPEEK, which strengthens the SPEEK polymer chains. To further co-relate the above data, fuel cross-over and EIS for the membranes was performed at regular interval of ADT.

The gas permeability (H_2 fuel cross-over) measurement was carried out to understand the amount of fuel cross-over from anode to cathode during durability test. From Fig. 13b, it was found that the H_2 cross-over current density for pristine SPEEK was 0.87 mA cm^{-2} before the durability test and after 50 h of durability test it was found to be 5.08 mA cm^{-2} and finally after 100 h, it was 11.52 mA cm^{-2}. Whereas for SPEEK/sGNR (0.1 wt%) nanocomposite membrane shown in Fig. 13c, interestingly there is no significant H_2 cross-over current density before and after 100 h durability which is in the range of 0.74 mA cm^{-2}. Further it was observed that the nanocomposite membrane has no significant H_2 cross-over current density up to the 175 h of ADT. However, the H_2 cross-over has increased after 200 h of ADT and the value is 4.63 mA cm^{-2} (inset to Fig. 13c), which is lesser in comparison to the value of 11.52 mA cm^{-2} for pristine SPEEK discussed above. It is confirmed that the H_2 cross-over is very less for SPEEK/sGNR (0.1 wt%) nanocomposite membrane in comparison to pristine SPEEK may be due to the additive dispersion in the voids of the SPEEK matrix that restricts the cross-over and the molecules are made to traverse through the tortuous path. Hence sharp degradation in OCV for pristine SPEEK compared to SPEEK/sGNR (0.1 wt%) nanocomposite membrane can also be correlated with the high amount of fuel cross-over.

The EIS measurement for the pristine SPEEK and SPEEK/sGNR (0.1 wt%) nano-composite membrane was performed during the ADT to understand the membrane resistance and interfacial resistance in fuel cell mode. Nyquist plot shown in Fig. 13d and e before and after 100 h durability, suggest the high frequency resistance (HFR) on real axis of SPEEK/sGNR (0.1 wt%) nanocomposite membrane has shown lesser membrane resistance compared to the pristine SPEEK leading to improved PEFC performance for the composite.

4. Conclusions

Simultaneous unzipping and sulfonation of MWCNTs to form sGNR has shown enhanced dispersion and functional compatibility in the SPEEK matrix as a composite polymer electrolyte membrane. These composite membranes of SPEEK/sGNR show better water uptake and IEC which in turn helps in facile proton transport concomitant with increased proton conductivity. Mechanical stability of the SPEEK/sGNR (0.1 wt%) nanocomposite membrane is improved in comparison to pristine SPEEK. The MEAs comprising these membranes display better PEMFC performance in comparison with pristine SPEEK based MEAs. For example, in a fuel cell test bed, the SPEEK/sGNR (0.1 wt%) shows a current density of 840 mA cm^{-2} at 0.6 V (peak power density of 660 mW cm^{-2}) compared to the pristine SPEEK of 480 mA cm^{-2} at 0.6 V (peak power density of 331 mW cm^{-2}). Both the values are 1.7 times more than that of the measured values for pristine SPEEK membrane under similar conditions. Accelerated durability test suggest the higher durability of the nanocomposite membrane when compared to pristine SPEEK membrane. These results could pave the way for the application of sGNR as effective additive in different polymers to form cheaper and more durable composite polymer electrolyte membranes in fuel cell applications.

Acknowledgments

Mr. Avanish Shukla thank Council of Scientific and Industrial Research (CSIR), India and University Grants Commission (UGC), India for the CSIR-UGC fellowship (under UGC Fellowship Scheme). Dr. Santoshkumar D. Bhat thank the project under CSIR-Young Scientist Award Research Grant (DU-MLP-0090) for the funding.

Appendix A. Supporting information

Supplementary data associated with this article can be found in the online version at http://dx.doi.org/10.1016/j.memsci.2016.08.019.

References

[1] J.H. Chang, J.H. Park, G.G. Park, C.S. Kim, O.O. Park, Proton-conducting composite membranes derived from sulfonated hydrocarbon and inorganic materials, J. Power Sources 124 (2003) 18–25.
[2] T.J. Peckham, J. Schmeisser, S. Holdcroft, Relationships of acid and water content to proton transport in statistically sulfonated proton exchange membranes: variation of water content via control of relative humidity, J. Phys. Chem. B 112 (2008) 2848–2858.
[3] S.M.J. Zaidi, S.D. Mikhailenko, G.P. Robertson, M.D. Guiver, S. Kaliaguine, Proton conducting composite membranes from polyether ether ketone and heteropolyacids for fuel cell applications, J. Membr. Sci. 173 (2000) 17–34.
[4] J. Xu, S. Xu, P. Munroe, Z.-H. Xie, A. ZrN, Nanocrystalline coating for polymer electrolyte membrane fuel cell metallic bipolar plates prepared by reactive sputter deposition, RSC Adv. 5 (2015) 67348.
[5] H. Su, S. Pasupathi, B. Bladergroen, V. Linkov, B.G. Pollet, Performance investigation of membrane electrode assemblies for high temperature proton exchange membrane fuel cell, J. Power Energy Eng. 1 (2013) 95–100.
[6] S. Litster, G. McLean, PEM fuel cell electrodes, J. Power Sources 130 (2004) 61–76.
[7] M. Patri, V.R. Hande, S. Phadnis, B. Somaiah, S. Roychoudhury, P.C. Deb, Synthesis and characterization of SPE membrane based on sulfonated FEP-g-acrylic acid by radiation induced graft copolymerization for PEM fuel cell, Polym. Adv. Technol. 15 (2004) 270–274.
[8] N. Nishad Fathima, R. Aravindhan, D. Lawrence, U. Yugandhar, T.S.R. Moorthy, B. Unni Nair, SPEEK polymeric membranes for fuel cell application and their characterization: a review, J. Sci. Ind. Res. 66 (2007) 209–219.
[9] H. Dogan, E. Yildiz, M. Kaya, T.Y. Inan, Sulfonated carbon black based composite membranes for fuel cell applications, Bull. Mater. Sci. 36 (2013) 563–573.
[10] P. Knauth, H. Hou, E. Bloch, E. Sgreccia, M.L. Di Vona, Thermogravimetric analysis of SPEEK membranes: thermal stability, degree of sulfonation and cross-linking reaction, J. Anal. Appl. Pyrolysis 92 (2011) 361–365.
[11] Y. Wei, X. Ling, L. Zou, D. Lai, H. Lu, Y. Xu, A facile approach toward preparation of sulfonated multi-walled carbon nanotubes and their dispersibility in various solvents, Colloids Surf. A: Physicochem. Eng. Asp. 482 (2015) 507–513.
[12] R. Kannan, B.A. Kakade, V.K. Pillai, Polymer electrolyte fuel cells using Nafion-based composite membranes with functionalized carbon nanotubes, Angew. Chem. Int. Ed. 47 (2008) 2653–2656.
[13] N.P. Cele, S.S. Ray, S.K. Pillai, M. Ndwandwe, S. Nonjola, L. Sikhwivhilu, M. K. Mathe, Carbon nanotubes based Nafion composite membranes for fuel cell applications, Fuel Cells 10 (2010) 64–71.
[14] G. He, J. Zhao, S. Hu, L. Li, Z. Li, Y. Li, et al., Functionalized carbon nanotube via distillation precipitation polymerization and its application in Nafion-based composite membranes, ACS Appl. Mater. Interfaces 6 (2014) 15291–15301.
[15] R. Kannan, M. Parthasarathy, S.U. Maraveedu, S. Kurungot, V.K. Pillai, Domain size manipulation of perflourinated polymer electrolytes by sulfonic acid-functionalized MWCNTs to enhance fuel cell performance, Langmuir 25 (2009) 8299–8305.
[16] B. Guo, S.W. Tay, Z. Liu, L. Hong, Assimilation of highly porous sulfonated carbon nanospheres into Nafion matrix as proton and water reservoirs, Int. J. Hydrog. Energy 37 (2012) 14482–14491.
[17] H.-C. Chien, L.-D. Tsai, C.-P. Huang, C.-Y. Kang, J.-N. Lin, F.-C. Chang, Sulfonated graphene oxide/Nafion composite membranes for high-performance direct methanol fuel cells, Int. J. Hydrog. Energy 38 (2013) 13792.
[18] Z. Jiang, X. Zhao, Y. Fu, A. Manthiram, Composite membranes based on sulfonated poly(ether ether ketone) and SDBS-adsorbed graphene oxide for direct methanol fuel cells, J. Mater. Chem. 22 (2012) 24862.
[19] G. Rambabu, S.D. Bhat, Sulfonated fullerene in SPEEK matrix and its impact on the membrane electrolyte properties in direct methanol fuel cells, Electrochim. Acta 176 (2015) 657–669.
[20] D.B. Shinde, M. Majumder, V.K. Pillai, Counter-ion dependent, longitudinal unzipping of multi-walled carbon nanotubes to highly conductive and transparent graphene nanoribbons, Sci. Rep. 4 (2014) 4363.
[21] G. Rambabu, S.D. Bhat, Simultaneous tuning of methanol crossover and ionic conductivity of sPEEK membrane electrolyte by incorporation of PSSA functionalized MWCNTs: a comparative study in DMFCs, Chem. Eng. J. 243 (2014) 517–525.

[22] S. Sasikala, S. Meenakshi, S.D. Bhat, A.K. Sahu, Functionalized bentonite clay-sPEEK based composite membranes for direct methanol fuel cells, Electrochim. Acta 135 (2014) 232–241.
[23] B. Annapurna, S. Meenakshi, S.D. Bhat, S. Seshadri, Microbial extracellular polysaccharide-based membrane in polymer electrolyte fuel cells, Chem. Eng. J. 231 (2013) 373–379.
[24] J. Fan, Z. Shi, M. Tian, J. Wang, J. Yin, Unzipped multiwalled carbon nanotube oxide/multiwalled carbon nanotube hybrids for polymer reinforcement, ACS Appl. Mater. Interfaces 4 (2012) 5956–5965.
[25] L. Jiao, X. Wang, G. Diankov, H. Wang, H. Dai, Facile synthesis of high-quality graphene nanoribbons, Nat. Nanotechnol. 5 (2010) 321–325.
[26] A.K. Gupta, T.J. Russin, H.R. Gutiérrez, P.C. Eklund, Probing graphene edges via raman scattering, ACS Nano 3 (2009) 45–52.
[27] M.S. Dresselhaus, G. Dresselhaus, R. Saito, A. Jorio, Raman spectroscopy of carbon nanotubes, Phys. Rep. 409 (2005) 47–99.
[28] Z. Ni, Y. Wang, T. Yu, Z. Shen, Raman spectroscopy and imaging of graphene, Nano Res. 1 (2008) 273–291.
[29] X.-L. Ling, Y.-Z. Wei, L.-M. Zou, S. Xu, Preparation and characterization of hydroxylated multi-walled carbon nanotubes, Colloids Surf. A: Physicochem. Eng. Asp. 421 (2013) 9–15.
[30] L. Stobinski, B. Lesiak, L. Kover, J. Toth, S. Biniak, G. Trykowski, J. Judek, Multiwall carbon nanotubes purification and oxidation by nitric acid studied by the FTIR and electron spectroscopy methods, J. Alloy. Compd. 501 (2010) 77–84.
[31] Y. Wang, Z. Iqbal, S. Mitra, Rapidly functionalized, water-dispersed carbon nanotubes at high concentration, J. Am. Chem. Soc. 128 (2006) 95–99.
[32] C.Y. Du, T.S. Zhao, Z.X. Liang, Sulfonation of carbon-nanotube supported platinum catalysts for polymer electrolyte fuel cells, J. Power Sources 176 (2008) 9–15.
[33] Q.H. Li, S.X. Chen, L.Z. Zhuang, X.Z. Xu, H.C. Li, Preparation of a sulfonated activated carbon fiber catalyst with gamma-irradiation-induced grafting method, J. Mater. Res. 27 (2012) 3083–3089.
[34] V. Datsyuk, M. Kalyva, K. Papagelis, J. Parthenios, D. Tasis, A. Siokou, et al., Chemical oxidation of multiwalled carbon nanotubes, Carbon 46 (2008) 833–840.
[35] H. Naeimi, M. Dadaei, Functionalized multi-walled carbon nanotubes as an efficient reusable heterogeneous catalyst for green synthesis of N-substituted pyrroles in water, RSC Adv. 5 (2015) 76221.
[36] L.C. Scienza, G.E. Thompson, Preparation and surface analysis of PPY/SDBS films on aluminum substrates, Polím.: Ciênc. Tecnol. 11 (2001) 142–148.
[37] S.R. Taffarel, J. Rubio, Adsorption of sodium dodecyl benzene sulfonate from aqueous solution using a modified natural zeolite with CTAB, Miner. Eng. 23 (2010) 771–779.
[38] L. Zhang, Y. Hashimoto, T. Taishi, Q.Q. Ni, Mild hydrothermal treatment to prepare highly dispersed multi-walled carbon nanotubes, Appl. Surf. Sci. 257 (2011) 1845–1849.
[39] S. Mallakpour, A. Zadehnazari, One-pot synthesis of glucose functionalized multi-walled carbon nanotubes: dispersion in hydroxylated poly(amide-imide) composites and their thermo-mechanical properties, Polymer 54 (2013) 6329–6338.
[40] P. Staiti, F. Lufrano, A.S. Arico, E. Passalacqua, V. Antonucci, Sulfonated polybenzimidazole membranes - preparation and physico-chemical characterization, J. Membr. Sci. 188 (2001) 71–78.
[41] F. Wang, M. Hickner, Y.S. Kim, T.A. Zawodzinski, J.E. McGrath, Direct polymerization of sulfonated poly(arylene ether sulfone) random (statistical) copolymers: candidates for new proton exchange membranes, J. Membr. Sci. 197 (2002) 231–242.
[42] X. Li, D. Chen, D. Xu, C. Zhao, Z. Wang, H. Lu, H. Na, SPEEKK/polyaniline (PANI) composite membranes for direct methanol fuel cell usages, J. Membr. Sci. 275 (2006) 134–140.
[43] Y. Jin, S. Qiao, L. Zhang, Z.P. Xu, S. Smart, J.C.D. da Costa, et al., Novel Nafion composite membranes with mesoporous silica nanospheres as inorganic fillers, J. Power Sources 185 (2008) 664–669.
[44] K.D. Kreuer, On the development of proton conducting polymer membranes for hydrogen and methanol fuel cells, J. Membr. Sci. 185 (2001) 29–39.
[45] M. Saito, K. Hayamizu, T. Okada, Temperature dependence of ion and water transport in perfluorinated ionomer membranes for fuel cells, J. Phys. Chem. B 109 (2005) 3112–3119.